JPET Fast Forward. Published on October 18, 2007 as DOI: 10.1124/jpet.107.127704

Quantitation of doxorubicin uptake, efflux and modulation of multidrug resistance (MDR) in MDR human cancer cells

Fei Shen, Shaoyou Chu, Aimee K. Bence, Barbara Bailey, Xinjian Xue, Priscilla A. Erickson, Marshall H. Montrose, William T. Beck, and Leonard C. Erickson

Indiana University Cancer Center, Department of Pharmacology and Toxicology (F.S., A.K.B., B.B., X.X., P.A.E., L.C.E), and Department of Cellular and Integrative Physiology (S.C., M. H. M.), Indiana University School of Medicine, Indianapolis, Indiana; and Department of Biopharmaceutical Sciences (W.T.B.), University of Illinois at Chicago, Chicago, Illinois

Quantitation of MDR and its modulation in MDR cancer cells

Corresponding Author:

Leonard C. Erickson, PhD

Indiana Cancer Center

Cancer Research Institute, R4-Rm 168

1044 West Walnut St

Indianapolis, IN 46202

(317) 274-5202

(317) 274 8046

lcericks@iupui.edu

The number of text pages: 23

The number of Tables: 2

The number of figures: 6

The number of references: 28

The number of words in the Abstract: 219

The number of words in the Introduction: 626

The number of words in the Discussion: 1217

ABBREVIATIONS: MDR, Multidrug resistance; DOX, doxorubicin; CsA, cyclosporine A; Verp, verapamil.

Abstract

P-glycoprotein, a membrane transporter encoded by the MDR1 gene in human cells, mediates drug efflux from cells and plays a major role in causing MultiDrug Resistance (MDR). Confocal microscopy was used to study *in vitro* and *in vivo* drug accumulation, net uptake and efflux, and MDR modulation by P-glycoprotein inhibitors in MDR1-transduced human MDA-MB-435mdr (MDR) cancer cells. The MDR cells were about nine fold more resistant to the anticancer drug doxorubicin than their parental wild type MDA-MB-435wt (WT) cells. Doxorubicin accumulation in the MDR cells was only 19% of that in the WT cells. The net uptake of doxorubicin in the nuclei of the MDR cells was two-fold lower than that in the nuclei of the WT cells. Pgp inhibitors, verapamil, cyclosporine A, or PSC833 increased doxorubicin accumulation in the MDR cells up to 79%, and reversed drug resistance in these cells. In living animals, doxorubicin accumulation in MDA-MB-435mdr xenograft tumors was 68% of that in the wild type tumors. Administration of verapamil, cyclosporine A, or PSC833 prior to doxorubicin treatment of the animals increased doxorubicin accumulation in the MDR tumors up to 94%. These studies have added direct *in vitro* and *in vivo* information on the capacity of the transporter protein Pgp to efflux doxorubicin and on the reversal of MDR by Pgp inhibitors in resistant cancer cells.

Introduction

Drug resistance is a significant factor that limits the effectiveness of current chemotherapeutic drugs. Although resistance can develop through a wide variety of mechanisms, multidrug resistance due to the overexpression of drug transporters such as p-glycoprotein (Pgp) is an established cause of drug resistance (Broxterman et al., 1995). Pgp is a transmembrane protein encoded by the MDR1 gene in human cells. As a member of the ABC family of drug transporters, Pgp effluxes a wide variety of hydrophobic, neutral, and positively charged drugs from the cell. Pgp expression is a component of the normal cellular defense system against xenobiotics (Gottesman et al., 2002). However, in some human cancers the overexpression of Pgp is correlated with decreased survival and poor prognosis (Diestra et al., 2003; Leonessa and Clarke, 2003).

Intracellular drug accumulation is a complex process comprised of drug uptake into the cell, retention and distribution in the cell, and efflux from the cell. At any given time point the net uptake (accumulation) of a drug in cells is the difference between the amount of drug uptake and efflux. Pgp mediating drug efflux decreases intracellular net drug uptake and causes cells to be drug resistant. In an attempt to overcome the resistance that can develop due to Pgp overexpression, Pgp inhibitors have been developed (Teodori et al., 2006). The rationale to develop inhibitors is straightforward; it is hypothesized that if the action of Pgp (drug efflux) is blocked, it will result in an increased net uptake of drugs and greater clinical efficacy of chemotherapeutic agents in tumors overexpressing Pgp. First generation inhibitors included drugs such as cyclosporine A, quinidine, tamoxifen, and verapamil (Ferry et al., 1996). Although these drugs were active inhibitors of Pgp, they were not sufficiently active *in vivo* and

the doses required for inhibition of Pgp resulted in other pharmacologic activity that led to unacceptable toxicity. Consequently, more specific and effective inhibitors were developed. Second generation inhibitors including dexverapamil, PSC-833 (valspodar), and biricodar (VX-710), however, altered the pharmacokinetics of the chemotherapeutic agents necessitating dose reductions (Rowinsky et al., 1998). A variety of third generation Pgp inhibitors are currently in clinical development including tarquidar, zosuquidar, elacridar, laniquidar, lonafarnib and ONT-093 (Thomas and Coley, 2003; Jabbour et al., 2004). Several of these compounds have entered phase III clinical trials (Gerrard et al., 2004). However, some of these agents have had disappointing results (Doll et al., 2004; Pusztai et al., 2005), and the future clinical development of others is in jeopardy.

Over the last 15 years there have been over 150 clinical trials with approximately 30 different inhibitors, but a Pgp inhibitor has yet to be approved by the FDA (Oza, 2002). The outcome suggests that improved preclinical screening of potential inhibitors would be a valuable contribution to improving agent selection for clinical trials. This improvement would not only better utilize the resources available for clinical studies, but may also prevent patients from participating in an unsuccessful clinical trial. Although there are a wide variety of assays for determining the intracellular accumulation and efflux of drugs mediated by Pgp and for evaluating the effectiveness of Pgp inhibitors, only a limited number of techniques allow for direct visualization and assessment of these processes. Of the techniques, confocal microscopy is a widely used and valuable tool for these studies.

Studies on drug accumulation in cultured resistant cancer cells have been published by other investigators, however, studies on visualizing in real time how Pgp processes anticancer drugs and how Pgp inhibitors modulate MDR *in vitro and in vivo* have not been reported. This paper presents studies using confocal microscopy to visualize and assess doxorubicin net uptake and efflux *in vitro*, and to evaluate the effectiveness of first and second-generation Pgp inhibitors in modulating drug efflux *in vitro* and *in vivo*.

JPET Fast Forward. Published on October 18, 2007 as DOI: 10.1124/jpet.107.127704
This article has not been copyedited and formatted. The final version may differ from this version.

Materials and Methods

Reagents, Cell lines and Animals

Doxorubicin hydrochloride, verapamil and cyclosporine A were purchased from Sigma (St. Loius, MO). PSC833 was a gift to W.T.B. from Dalia Cohen (Novartis Pharmaceuticals, Florham Park, NJ). Stock solutions were made by dissolving doxorubicin (Bouhadir et al., 2001) and verapamil in saline, and cyclosporine A and PSC833 in DMSO, and were stored at -20^{O}C until use. The final concentration of DMSO in the treated cells was less than 0.1%. Cyclosporine A and PSC833 were also dissolved in the vehicle of 7:3 sterile water to 95% ethanol for animal injections (Hermanussen et al., 2004).

Wild type MDA-MB-435 human cancer cells (MDA-MB-435wt) and the MDA-MB-435 cells retrovirally transduced with the MDR1 gene to express Pgp (MDA-MB-435mdr, MDR cells) were obtained from Dr. George Sledge (Indiana University). MDA-MB-435 cells were widely accepted previously as human breast cancer cells. However, some investigators have recently suggested that this cell line may have originated from a melanoma (Ellison et al., 2002). MDA-MB-435 cells were grown in Alpha MEM with 10% bovine calf serum (Hyclone, Provo, Utah), 1 mM glutamine and 2mM sodium pyruvate (Gemini BioProducts, Calabasas, CA), 100 U/ml penicillin and 100 U/ml and 100 U/ml streptomycin (Gibco/BRL, Gaithersburg, MD).

Animal studies were carried out with protocols approved by the Animal Care and Use Committee of Indiana University. Female nude/nude mice, 6-8 weeks of age were injected subcutaneously with human MDA-MB-435 cancer cells. Each mouse was injected with $15x10^6$ MDA-MB-435wt cells on one flank, and with $15x10^6$ MDA-MB-435mdr cells on the other

flank. The injection produced a palpable tumor within 3-4 weeks. Confocal image studies were then conducted on the mice.

Western Blot Analysis of Pgp expression

Cell lysates used for western blot analysis were prepared from crude cell membranes following established procedures (Pincheira et al., 2001). Briefly, cells were harvested, washed and centrifuged. The pellet was resuspended in hypotonic lysis buffer, and centrifuged at 4000 x g to remove cell debris. The supernatant from the second centrifugation was retained and centrifuged again to obtain crude cell membranes which were then resuspended in sucrose buffer and used as lysates for western blot.

Protein concentration in the cell lysates was determined with the Bradford Assay, and equal amounts of proteins loaded on gels. Cell lysates were separated by SDS-PAGE and transferred to a PVDF membrane. The blot was then probed with primary monoclonal antibody C219 (dilution 1:1000) (ID Labs Biotechnology, Ontario, Canada), followed by reaction with HRP-conjugated secondary antibody. The signal was detected using enhanced chemluminensence (ECL) and exposure of x-ray film.

Cytotoxicity of doxorubicin and reversal of MDR by Pgp inhibitors

Colony formation assay was used to evaluate doxorubicin cytotoxicity and the reversal of resistance by Pgp inhibitors. A total of 3×10^5 cells were seeded in 5 ml of culture medium in each 25-cm^2 flask and incubated under standard conditions for 24 h. Each flask of cells was treated with a different dose of doxorubicin for 1 h. To assess the reversal of MDR by Pgp inhibitors, the cells were pretreated with verapamil, cyclosporine A, or PSC833 30 min prior to doxorubicin exposure. The cells were then washed with PBS, trypsinized, counted, and seeded

into triplicate 100-mm cell culture dishes at densities of 500 and 750 cells/dish in culture medium. After incubation under standard conditions for 14 days, colonies were fixed with methanol, stained with 10% methylene blue in PBS, and visually counted.

Doxorubicin intracellular distribution, accumulation and their modulation by Pgp inhibitors

MDA-MB-435 cells were seeded on cover slips in 6-well plates and allowed to grow overnight. On the following day, cells were washed with PBS, incubated with or without 5μM verapamil, 2.5 μM cyclosporine A, or 3 mg/ml PSC833 for 30 min before treatment with 5 μM doxorubicin for two hours, and then examined using confocal microscopy.

Dynamic assessment of doxorubicin net uptake, efflux and effects of Pgp inhibitors

MDA-MB-435 cells were seeded on cover slips overnight. The cover slips were mounted in microscope chambers which were placed on the microscope stage and perfused sequentially with doxorubicin-free medium for six minutes, medium with 5 μM doxorubicin for two hours (uptake perfusion), and then doxorubicin-free medium again for one hour (efflux perfusion). Serial images at one-minute intervals were collected and analyzed. To study the effect of Pgp inhibitors on the time course of doxorubicin accumulation and efflux, MDA-MB-435mdr cells grown on cover slips were pre-exposed to 5 μM verapamil, 2.5 μM cyclosporine A, or 3 mg/ml PSC833 for 30 minutes before being mounted in microscope chambers for perfusion as described above.

Doxorubicin accumulation and effects of Pgp inhibitors in tumor xenografts in living nude mice

Living nude mice bearing subcutaneous MDA-MB-435 wt and MDA-MB-435mdr tumor xenografts on opposite flanks were injected with 4, 8 or 16 mg/kg doxorubicin intravenously. In order to study the effect of Pgp inhibitors, tumor bearing mice were administered with or without 10mg/kg verapamil, 50 mg/kg cyclosporine or 50 mg/kg PSC833 intraperitoneally one hour prior

to receiving intravenous injection of 8mg/kg doxorubicin. Confocal tumor images were taken two hours after the mice had received doxorubicin. To obtain the images, the mice were anesthetized and a small skin incision was made to expose the xenografts. The mice were placed on the microscope stage connected to a water circulator set to 37^{O}C.

Confocal Microscopy and image analysis

Images were collected using an LSM510 NLO confocal microscope with a C-Apo X40 water immersion lens (Karl Zeiss, Jena, Germany). Doxorubicin fluorescence was excited with an Argon laser at 488nM, and the emission collected through a 530nM long-pass filter. The same confocal settings (excitation, laser power, detector gain and pinhole size) were used to image the wild type and the MDR cells *in vitro* and the wild type and MDR xenograft tumors *in vivo*. Post data-acquisition image analysis was performed using MetaMorph^{TM}, software (Universal Imaging, Downingtown, PA). Cell images were analyzed as mean doxorubicin fluorescent intensity per pixel in a circular 314 pixel region of the nucleus or cytoplasm of the same cell (approximately 60 μm^2). Multiple fields containing at least 15 cells/field were imaged in each experiment. The tumor images were analyzed as mean doxorubicin fluorescent intensity per pixel in a circular 785 pixel region of the tumor. Three regions of each tumor were randomly picked for image analysis. Results were obtained from analyzing images from three to five experiments.

Statistics

All data are expressed as mean ± SE from three or more experiments and statistically evaluated by Student's t test. Differences were considered significant when $p<0.05$.

JPET Fast Forward. Published on October 18, 2007 as DOI: 10.1124/jpet.107.127704
This article has not been copyedited and formatted. The final version may differ from this version.

Results

Pgp expression and resistance to doxorubicin

The expression of Pgp in MDA-MB-435 cells was demonstrated with western blot analysis (Fig.1). Monoclonal antibody C219 specifically detected a 180 kDa P-glycoprotein. The additional bands of lower molecular weight detected by the antibody represent degraded products of Pgp. The expression of Pgp was not detected in the wild type MDA-MB-435wt cells, but was observed in human MDA-MB-435mdr cancer cells. MDA-MB-435mdr cells had only a modest level of Pgp expression compared to the vinblastine-selected $SKOV_3$ cells used as the positive control in the western blot analysis.

The IC_{50} values of doxorubicin toxicity in MDA-MB-435wt cells and MDA-MB-435mdr cells were 0.60 ± 0.04 μM (Mean ± SE) and 5.29 ± 0.85 μM, respectively (Table 1). These results indicate that MDA-MB-435mdr cells were approximately nine times more resistant to doxorubicin than MDA-MB-435wt cells, despite the modest expression of Pgp in these cells.

Reversal of the resistance to doxorubicin by Pgp inhibitors

Pretreatment with verapamil, cyclosporine A, or PSC833 decreased the IC_{50} of doxorubicin toxicity in MDA-MB-435mdr cells to 2.41 ± 0.43 μM, 3.24 ± 0.26 μM or 3.71 ± 0.47 μM (Table 1), respectively, and reduced the IC_{50} of doxorubicin in MDR cells. The pretreatment with Pgp inhibitors had no significant effect on the IC_{50} of doxorubicin in MDA-MB-435wt type cells.

Doxorubicin intracellular distribution and accumulation

Confocal cell images were used to determine intracellular doxorubicin localization and accumulation in MDA-MB-435wt and MDA-MB-435mdr cells. Most wild type cells collected doxorubicin specifically in their nuclei. However, MDR cells accumulated doxorubicin in their

JPET Fast Forward. Published on October 18, 2007 as DOI: 10.1124/jpet.107.127704
This article has not been copyedited and formatted. The final version may differ from this version.

nuclei and cytoplasm. In addition, the MDR cells showed much weaker doxorubicin-related fluorescent intensity than the wild type cells (Fig. 2).

Effects of Pgp inhibitors on doxorubicin intracellular distribution and accumulation

Pretreatment of MDA-MB-435mdr cells with Pgp inhibitors re-localized doxorubicin to the nuclei and significantly increased the drug accumulation in these cells. In non-pretreated MDR cells doxorubicin fluorescent intensity was significantly low and amounted to only 19% of that in MDA-MB-435wt cells. Pretreatment with verapamil, cyclosporine A, or PSC833 increased doxorubicin accumulation in the MDR cells to 79%, 73% and 66% of that in the wild type cells, respectively (Fig. 3). The Pgp inhibitors had no significant effects on the intracellular distribution or accumulation of doxorubicin in the wild type cells (data not shown).

Dynamic assessment of doxorubicin net uptake and efflux in cytoplasm and nuclei of MDA-MB-435 cells

Sequential cell images were used to assess and compare the real time net uptake and efflux of doxorubicin in the nuclei and cytoplasm of MDA-MB-435wt and MDA-MB-435mdr cells. In both types of cells, the accumulation of doxorubicin differed markedly in the nuclei (Fig. 4A) but was similar in the cytoplasm (Fig. 4B). Nuclear net uptake of doxorubicin in the MDR cells was slower than that in the wild type cells, and at the end of two-hour doxorubicin uptake perfusion, drug accumulation in the nuclei of MDR cells was about two-fold less than that in the nuclei of wild type cells (Fig 4C). Doxorubicin efflux occurred immediately in the MDR and wild type cells after removal of doxorubicin from the perfusates. However, the efflux was faster in MDR cells than in the wild type cells. Doxorubicin efflux in the nuclei of MDR and wild type cells occurred at about the same rate (Fig. 4A) and led to a loss of 30% and 20% doxorubicin accumulation in the nuclei of MDR and wild type cells, respectively (Fig 4D). In contrast, in the

cytoplasm of MDR cells, the efflux quickly reduced doxorubicin accumulation to near baseline levels (Fig. 4B) and caused a loss of 47% of cytoplasmic doxorubicin accumulation at the end efflux perfusion. In the cytoplasm of wild type cells, a much slower efflux was observed with a loss of only 17 % cytoplasm doxorubicin accumulation (Fig. 4D). Because of the lower doxorubicin net uptake in their nuclei and stronger drug efflux in their cytoplasm, the MDR cells quickly and almost completely removed intracellular doxorubicin.

Effects of Pgp inhibitors on doxorubicin net uptake and efflux in cytoplasm and nuclei of MDA-MB-435mdr cells

Increased doxorubicin net uptake and decreased drug efflux were observed in MDA-MB-435mdr cells pretreated with Pgp inhibitors. At the end of the two-hour uptake perfusion, the fluorescent intensity of doxorubicin in the nuclei of the non-pretreated MDR cells was 1.8-fold of the baseline level. Pretreatment with verapamil, cyclosporine A and PSC833 increased the intensity to 4.6-, 3.4- and 3.4- fold, respectively (Fig. 4C). Increased doxorubicin accumulation in cytoplasm of pretreated MDR cells was also observed under the same conditions. Compared to the non-pretreated MDR cells, increased doxorubicin retention at the end of efflux perfusion was observed in the nuclei and cytoplasm of the MDR cells pretreated with verapamil and PSC833 (Fig. 4D). Surprisingly, cyclosporine A only increased uptake of doxorubicin but reduced its retention in MDR cells.

Doxorubicin accumulation in xenograft tumors in living mice

Confocal tumor images were used to evaluate *in vivo* doxorubicin accumulation and the effect of Pgp inhibitors on the accumulation in MDA-MB-435mdr tumors. Images of the tumors demonstrated similar distribution of doxorubicin in MDR and wild type tumor cells. Doxorubicin in both types of tumors was located around the periphery of the nuclei (Fig. 5). Accumulation of

doxorubicin in both wild type and MDR tumors increased with the increase of dose of doxorubicin injected to animals (Fig. 6). However, the accumulation in the MDR tumors was only 71%, 64% and 57% of that in the wild type tumors, respectively, in the mice intravenously receiving 4, 8 and 16mg/kg doxorubicin ($P<0.05$).

Effects of Pgp inhibitors on doxorubicin accumulation in xenograft tumors in living mice

Increased doxorubicin fluorescent intensity in MDA-MB-435mdr xenograft tumors was observed in mice pre-administrated with verapamil, cyclosporine A, or PSC833. Verapamil, cyclosporine A, or PSC833 increased doxorubicin accumulation in the MDR tumors to 90%, 84% or 94% of that in the wild type tumors, respectively (Table 2). The pre-administration of these Pgp inhibitors to mice eliminated the significant difference in doxorubicin fluorescent intensity between the MDR and wild type tumors. In addition, verapamil and PSC833 significantly increases of doxorubicin accumulation in MDR tumors compared to the non-pretreated MDR cells..

Discussion

Failure of chemotherapy in cancer patients has been observed due to the presence and/or development of drug resistance. Potential resistance mechanisms in cancer patients are those involving the multidrug resistance phenotype, including expression of Pgp. Doxorubicin is a Pgp substrate frequently used in the clinic to treat cancer patients (e.g. breast cancer, ovarian cancer, Kaposi's sarcoma). In this study, we have taken the advantage of the innate fluorescence of doxorubicin to evaluate how wild type and genetically engineered resistant human cancer cells accumulate, distribute, and efflux doxorubicin, and to study how Pgp inhibitors reversal of multidrug resistance *in vitro* and *in vivo.* ABC transporters such as Multidrug Resistant Protein (MRP) and Breast Cancer Resistant Protein (BCRP) are also known to be involved in causing MDR in cancer cells (Sharma et al., 2003). However, the current study only focused on evaluating the role of Pgp in mediating doxorubicin transport and multidrug resistance.

MDR1-transduced human MDA-MB-435mdr cancer cell line was used in the study in order to make it more relevant for investigating clinically resistant tumors. MDA-MB-435mdr cells only have a modest resistance to doxorubicin compared to drug selected resistant cell lines, which appear to have much higher levels of resistance than actual clinical tumors. In addition, a clinically achievable dose of doxorubicin (5 μM) was used in the *in vitro* cell imaging studies (Rahman et al., 1990).

The observation that some MDR cells displayed altered intracellular distribution and accumulation of doxorubicin compared to their parental wild type cells is consistent with that reported by other investigators (Meschini et al., 1994) and may indicate that Pgp reduces

doxorubicin access to nuclear targets in the cells. A number of studies have shown that doxorubicin intercalates into DNA molecules. The binding of doxorubicin to DNA inhibits DNA polymerase and nucleic acid synthesis. In addition, doxorubicin stabilizes the cleavable complex between DNA and topoisomerase II enzyme subunits, resulting in the formation of protein-linked DNA double-strand breaks (De Beer et al., 2001; Cutts et al., 2003) .

To our knowledge this is the first report on directly visualizing and dynamically assessing doxorubicin net uptake, efflux and modulation of MDR by Pgp inhibitors in cell nuclei and cytoplasm. Trans-membrane protein Pgp is well known for mediating drug efflux and causing a reduction of intracellular drug accumulation, which explains the decreased net doxorubicin uptake and increased drug efflux in cytoplasm and nuclei of MDR cells. Compared to the same cell compartment of wild type cells, doxorubicin net uptake in the nuclei of MDR cells showed relatively more reduction than that in the cytoplasm. However, compared to the nuclei, the cytoplasm of the MDR cells lost a greater fraction of the accumulated doxorubicin during the efflux perfusion. In the wild type cells the extent of reduction of doxorubicin accumulation in nuclei and cytoplasm in the same period was about the same (Fig. 6B). The data suggest that the reduced total intracellular doxorubicin accumulation was mainly caused by decreased net drug uptake in the nuclei and increased drug efflux in the cytoplasm of MDR cells. The action of doxorubicin binding DNA in nuclei and the efflux of doxorubicin mediated by Pgp on cell membrane (Sharma et al., 2003) may explain, at least in part, the obvious decreases of drug net uptake in the nuclei and increase of drug efflux in the cytoplasm of MDR cells.

The modulation of Pgp activity to reverse MDR has been intensively studied. Inhibition of Pgp in MDR cells sensitizes the cells to chemotherapeutic drugs *in vitro* and *in vivo* (Tan et al., 2000). Combined therapy with MDR-related antineoplastic agents and inhibitors shrinks tumors and prolongs the life span in some animal models. Pgp inhibitors, verapamil, cyclosporine A, and PSC833, reverse MDR and restore intracellular accumulation of drugs in MDR cells possibly by competitively binding to Pgp with drugs and/or by causing conformational changes in the transport protein (Tsuruo et al., 1981; Rao and Scarborough, 1994). Our results indicate that the above three Pgp inhibitors mainly modulate MDR by reversing drug net uptake in the nuclei of MDR cells. The modulating potential of Pgp inhibitors on MDR reported by other investigators (Keller et al., 1992) indicated that PSC833 was most effective, followed by cyclosporine A and verapamil. This rank order does not agree with our data. The discrepancy may be partially due to the dual inhibitory effects of verapamil and cyclosporine A on Pgp and Multidrug Resistant Protein (MRP) and the specific inhibitory effects of PSC833 only on Pgp, which is supported by some investigators (Qadir et al., 2005). Indeed, modest MRP expression was found in MDA-MB-435mdr cells (data not shown). Cyclosporine A increased net drug uptake in both nuclei and cytoplasm like verapamil and PSC833, however, it surprisingly enhanced drug efflux (Fig. 6B). Morphological changes were observed in the MDR cells pre-treated with cyclosporine A at the end of efflux perfusion experiment. Cyclosporine A may have induced toxicity to the cells and damaged the cell membrane and in turn caused doxorubicin “leaking” out of MDR cells.

In order to minimize differences in drug presentation and physical characteristics between animals in the *in vivo* study, experiments were conducted in mice that carried wild type tumor on one flank and MDR tumor on the other flank. The approach to evaluate drug accumulation in

tumors on living animals makes the animal study more relevant to the clinical situation. A difference in intracellular doxorubicin distribution between *in vitro* wild type cell and *in vivo* wild type tumor images was observed. It is possible that the doxorubicin dose administered to mice did not lead to a plasma doxorubicin level of 5 μM (the concentration used to treat cells in the *in vitro* study). Although cell nuclei have been considered the main target of doxorubicin, many studies have demonstrated that doxorubicin can also interact with other subcellular targets, such as cytoskeleton and membranes (Molinari et al., 1990), which may account for the distribution of doxorubicin observed in this study.

The results of tumor confocal images demonstrated that the increase of doxorubicin accumulation in MDA-MB-435 tumors was proportional with the dose of doxorubicin injected to animal, which may suggest that *in vivo* confocal imaging approach can be used to facilitate identification of a MDR tumor phenotype and more importantly, and enables a screen for inhibitors of either MDR1 or other targets that increase of the accumulation doxorubicin in tumors.

This study showed that the increases of doxorubicin accumulation in MDR cells by Pgp modulators, verapamil, cyclosporine A and PSC833 *in vitro* was more apparent than that *in vivo*. The results may be explained, at least in part, that doses of inhibitors injected intrapritoneally in mice did not yielded a plasma concentration similar to that used to treat the cells *in vitro*. In future *in vivo* studies, monitoring the plasma concentration of these inhibitors in mice should be considered.

This paper provides direct information on the capacity of modest levels of the transporter protein Pgp to decrease intracellular drug accumulation *in vitro* and *in vivo*. The study developed a new approach to examine in real time how MDR cancer cells accumulate and efflux substrate anticancer drugs and respond to transport inhibitors. This new approach will facilitate drug uptake and efflux studies *in vitro* and *in vivo*, and may help the future development and evaluation of new inhibitors of MDR transporters.

References

Bouhadir KH, Alsberg E and Mooney DJ (2001) Hydrogels for combination delivery of antineoplastic agents. *Biomaterials* **22**:2625-2633.

Broxterman HJ, Giaccone G and Lankelma J (1995) Multidrug resistance proteins and other drug transport-related resistance to natural product agents. *Current Opinion in Oncology* **7**:532-540.

Cutts SM, Swift LP, Rephaeli A, Nudelman A and Phillips DR (2003) Sequence specificity of adriamycin-DNA adducts in human tumor cells. *Molecular Cancer Therapeutics* **2**:661-670.

De Beer EL, Bottone AE and Voest EE (2001) Doxorubicin and mechanical performance of cardiac trabeculae after acute and chronic treatment: a review. *European Journal of Pharmacology* **415**:1-11.

Diestra JE, Condom E, Del Muro XG, Scheffer GL, Perez J, Zurita AJ, Munoz-Segui J, Vigues F, Scheper RJ, Capella G, Germa-Lluch JR and Izquierdo MA (2003) Expression of multidrug resistance proteins P-glycoprotein, multidrug resistance protein 1, breast cancer resistance protein and lung resistance related protein in locally advanced bladder cancer treated with neoadjuvant chemotherapy: biological and clinical implications. *Journal of Urology* **170**:1383-1387.

Doll RJ, Kirschmeier P and Bishop WR (2004) Farnesyltransferase inhibitors as anticancer agents: critical crossroads. *Current Opinion in Drug Discovery & Development* **7**:478-486.

Ellison G, Klinowska T, Westwood RFR, Docter E, French T and Fox JC (2002) Further evidence to support the melanocytic origin of MDA-MB-435. *Molecular Pathology* **55**:294-299.

Ferry DR, Traunecker H and Kerr DJ (1996) Clinical trials of P-glycoprotein reversal in solid tumours. *European Journal of Cancer* **32A**:1070-1081.

Gerrard G, Payne E, Baker RJ, Jones DT, Potter M, Prentice HG, Ethell M, McCullough H, Burgess M, Mehta AB and Ganeshaguru K (2004) Clinical effects and P-glycoprotein inhibition in patients with acute myeloid leukemia treated with zosuquidar trihydrochloride, daunorubicin and cytarabine. *Haematologica* **89**:782-790.

Gottesman MM, Fojo T and Bates SE (2002) Multidrug resistance in cancer: role of ATP-dependent transporters. *Nature Reviews Cancer* **2**:48-58.

Hermanussen S, Do M and Cabot PJ (2004) Reduction of beta-endorphin-containing immune cells in inflamed paw tissue corresponds with a reduction in immune-derived antinociception: reversible by donor activated lymphocytes. *Anesthesia & Analgesia* **98**:723-729.

Jabbour E, Kantarjian H and Cortes J (2004) Clinical activity of farnesyl transferase inhibitors in hematologic malignancies: possible mechanisms of action. *Leukemia & Lymphoma* **45**:2187-2195.

Keller RP, Altermatt HJ, Nooter K, Poschmann G, Laissue JA, Bollinger P and Hiestand PC (1992) SDZ PSC 833, a non-immunosuppressive cyclosporine: its potency in overcoming P-glycoprotein-mediated multidrug resistance of murine leukemia. *International Journal of Cancer* **50**:593-597.

Leonessa F and Clarke R (2003) ATP binding cassette transporters and drug resistance in breast cancer. *Endocrine-Related Cancer* **10**:43-73.

Meschini S, Molinari A, Calcabrini A, Citro G and Arancia G (1994) Intracellular localization of the antitumour drug adriamycin in living cultured cells: a confocal microscopy study. *Journal of Microscopy* **176**:204-210.

Molinari A, Calcabrini A, Crateri P and Arancia G (1990) Interaction of anthracyclinic antibiotics with cytoskeletal components of cultured carcinoma cells (CG5). *Experimental & Molecular Pathology* **53**:11-33.

Oza AM (2002) Clinical development of P glycoprotein modulators in oncology. *Novartis Foundation Symposium* **243**:103-115; discussion 115-108.

Pincheira R, Chen Q and Zhang JT (2001) Identification of a 170-kDa protein over-expressed in lung cancers. *British Journal of Cancer* **84**:1520-1527.

Pusztai L, Wagner P, Ibrahim N, Rivera E, Theriault R, Booser D, Symmans FW, Wong F, Blumenschein G, Fleming DR, Rouzier R, Boniface G and Hortobagyi GN (2005) Phase II study of tariquidar, a selective P-glycoprotein inhibitor, in patients with chemotherapy-resistant, advanced breast carcinoma. *Cancer* **104**:682-691.

Qadir M, O'Loughlin KL, Fricke SM, Williamson NA, Greco WR, Minderman H and Baer MR (2005) Cyclosporin A is a broad-spectrum multidrug resistance modulator. *Clinical Cancer Research* **11**:2320-2326.

Rahman A, Treat J, Roh JK, Potkul LA, Alvord WG, Forst D and Woolley PV (1990) A phase I clinical trial and pharmacokinetic evaluation of liposome-encapsulated doxorubicin. *Journal of Clinical Oncology* **8**:1093-1100.

Rao US and Scarborough GA (1994) Direct demonstration of high affinity interactions of immunosuppressant drugs with the drug binding site of the human P-glycoprotein. *Molecular Pharmacology* **45**:773-776.

Rowinsky EK, Smith L, Wang YM, Chaturvedi P, Villalona M, Campbell E, Aylesworth C, Eckhardt SG, Hammond L, Kraynak M, Drengler R, Stephenson J, Jr., Harding MW and Von Hoff DD (1998) Phase I and pharmacokinetic study of paclitaxel in combination with biricodar, a novel agent that reverses multidrug resistance conferred by overexpression of both MDR1 and MRP. *Journal of Clinical Oncology* **16**:2964-2976.

Sharma R, Awasthi YC, Yang Y, Sharma A, Singhal SS and Awasthi S (2003) Energy dependent transport of xenobiotics and its relevance to multidrug resistance. *Current Cancer Drug Targets* **3**:89-107.

Tan B, Piwnica-Worms D and Ratner L (2000) Multidrug resistance transporters and modulation. *Current Opinion in Oncology* **12**:450-458.

Teodori E, Dei S, Martelli C, Scapecchi S and Gualtieri F (2006) The functions and structure of ABC transporters: implications for the design of new inhibitors of Pgp and MRP1 to control multidrug resistance (MDR). *Current Drug Targets* **7**:893-909.

Thomas H and Coley HM (2003) Overcoming multidrug resistance in cancer: an update on the clinical strategy of inhibiting p-glycoprotein. *Cancer Control* **10**:159-165.

Tsuruo T, Iida H, Hori K, Tsukagoshi S and Sakurai Y (1981) Membrane affinity and metabolism of N4-palmitoyl-1-beta-D-arabinofuranosylcytosine into cultured KB cells. *Cancer Research* **41**:4484-4488.

Footnotes

This study was supported by Grant CA96839-01 from the National Cancer Institute.

Requests for reprints: Leonard C. Erickson, Cancer Research Institute, R4-Rm 168, 1044 W. Walnut St, Indianapolis, IN 46202, lcericks@iupui.edu

Current address for Shaoyou Chu: Cellular Imaging Laboratory, Lead Generation/Optimization Biology, Lilly Research Laboratories, Lilly Corporate Center, Indianapolis, IN 46285

Current address for Marshall H. Montrose: Department of Molecular and Cellular Physiology, University of Cincinnati, 231 Albert Sabin Way, Cincinnati, OH 45267

Legends for Figures

Fig. 1. Western blot analysis of P-glycoprotein in human cancer cells. Lane 1: Vinblastin-selected SKOV3 cells (positive control); Lane 2 and 3: MDA-MB-435mdr cells; Lane 4: MDA-MB-435wt cells. Monoclonal antibody C219 specifically detected a 180 kDa P-glycoprotein. The additional bands of lower molecular weight detected by the antibody represent degraded products of Pgp.

Fig. 2. *In vitro* confocal images of sub-cellullar doxorubicin fluorescence distribution in parental human MDA-MB-435wt cells (upper) and drug resistant MDA-MB-435mdr cells (lower). (A) Confocal images (left); Nomarski Differential Interference Contrast (DIC) images (middle); overlays of confocal and DIC images (right). (B): Higher magnification of the boxed areas in A.

Fig. 3. *In vitro* confocal cells images (A) MDA-MB-435wt (upper) and MDA-MB-435mdr (lower) cells pre-treated with Pgp inhibitors for 30 min before 5uM doxorubicin added. (B) Doxorubicin accumulation in MDA-MB-435 cells pretreated or non-pretreated with Pgp inhibitors. Values are mean ± SE. * Significant difference ($p < 0.05$) of fluorescent intensity of doxorubicin in the wild type and in the MDR cells.

Fig. 4. Doxorubicin uptake and efflux in the nuclei (A) and cytoplasm (B) of MDA-B-435 cells. The experiments were performed as described in materials and methods. MDA-MB-435 cells pretreated or non-pretreated with Pgp inhibitors were perfused sequentially with medium,

medium containing doxorubicin (uptake perfusion), and then medium again (efflux perfusion). Serial images were collected and analyzed. Doxorubicin accumulation in the nuclei and cytoplasm of MDA-MB-435cells was assessed at the end of uptake (C) and efflux (D) perfusion. Fluorescent intensity of doxorubicin in cellular nuclei and cytoplasm at the end of uptake and efflux perfusion was calculated relative to that in the same cellular compartment at the baseline level and at end of uptake perfusion, respectively.

Fig. 5. *In vivo* confocal images of doxorubicin accumulation in MDA-MB-435wt tumor xenograft (upper) and drug resistant MDA-MB-435mdr tumor xenograft (lower). Confocal images (left); reflecting images (middle); overlays of confocal and reflecting images (right). The inset is an enlarged tumor image from the boxed area in the figure.

Fig. 6. Accumulation of doxorubicin in MDA-MB-435 wild type and MDR tumors in mice injected with 4, 8 and 16 mg/kg doxorubicin. Confocal tumor images were taken two hours after the mice had received doxorubicin. * Significantly difference with the wild type tumors ($p < 0.05$).

JPET Fast Forward. Published on October 18, 2007 as DOI: 10.1124/jpet.107.127704
This article has not been copyedited and formatted. The final version may differ from this version.

Table 1

Toxicity of doxorubicin and modulation of drug resistance by verapamil, cyclosporine A and PSC833 in human MDA-MB-435 cancer cells

Agent	IC50 (µM) MDA-MB-435wt cells	FS[a]	IC50 (µM) MDA-MB-435mdr cells	RF[b]	FS
Doxorubicin	0.60 ± 0.04	1.0	5.29 ± 0.85	8.8[c]	1.0
+ 5 µM verapamil	0.52 ± 0.03	1.2	2.41 ± 0.43	4.6[cd]	1.9
+ 2.5 µM CsA	0.53 ± 0.04	1.1	3.24 ± 0.26	6.1[cd]	1.4
+ 3 mg/ml PSC833	0.57 ± 0.04	1.1	3.71 ± 0.47	6.5[cd]	1.4

Cell toxicity was measured as described in methods, in response to increasing concentrations of doxorubicin.

[a]Fold sensitization was calculated as IC50 of doxorubicin cells divided by IC50 of doxorubicin in the same cells pretreated with Pgp inhibitors.

[b]Resistance factor was calculated as IC50 of doxorubicin in MDA-MB-435 cells divided by IC50 of the same drug in MDA-MB-435 cells pretreated with Pgp inhibitors.

[C]Statistically significant increase ($p < 0.05$) in resistance between the wild type and the MDR cell lines.

[d]Statistically significant decrease ($p < 0.05$) in resistance between the MDR cell line and the MDR cell line pretreated with Pgp inhibitors.

Table 2

Doxorubicin Accumulation in MDA-MB- 435 xenograft Tumors

Pre-injected with	Doxorubicin fluorescent intensity in WT tumor (Mean ± SE)	% of non-pretreated WT tumor	Doxorubicin fluorescent intensity in MDR tumor (Mean ± SE)	% of the WT tumor	% of non-pretreated MDR tumor
	75 ± 4.7	100	51 ± 6.0	68*	100
Verapamil	82 ± 6.5	109	74 ± 7.3	90	145**
Cyclosporine A	75 ± 5.1	100	65 ± 6.4	87	127
PSC833	80 ± 4.6	106	76 ± 6.3	94	149**

Mice were injected with or without 10mg/kg verapamil, 50 mg/kg cyclosporine or 50 mg/kg PSC833 intraperitoneally one hour prior to receiving intravenous injection of 8mg/kg doxorubicin. Confocal tumor images were taken two hours after the mice had received doxorubicin.

**Statistically significant difference ($p < 0.05$) in fluorescent intensity of doxorubicin in MDA-MB-435wt tumors and MDA-MB-435mdr tumors.*

***Statistically significant difference ($p < 0.05$) in fluorescent intensity of doxorubicin in non-pretreated MDA-MB-435mdr tumors and pre-treated MDA-MB-435mdr tumors.*

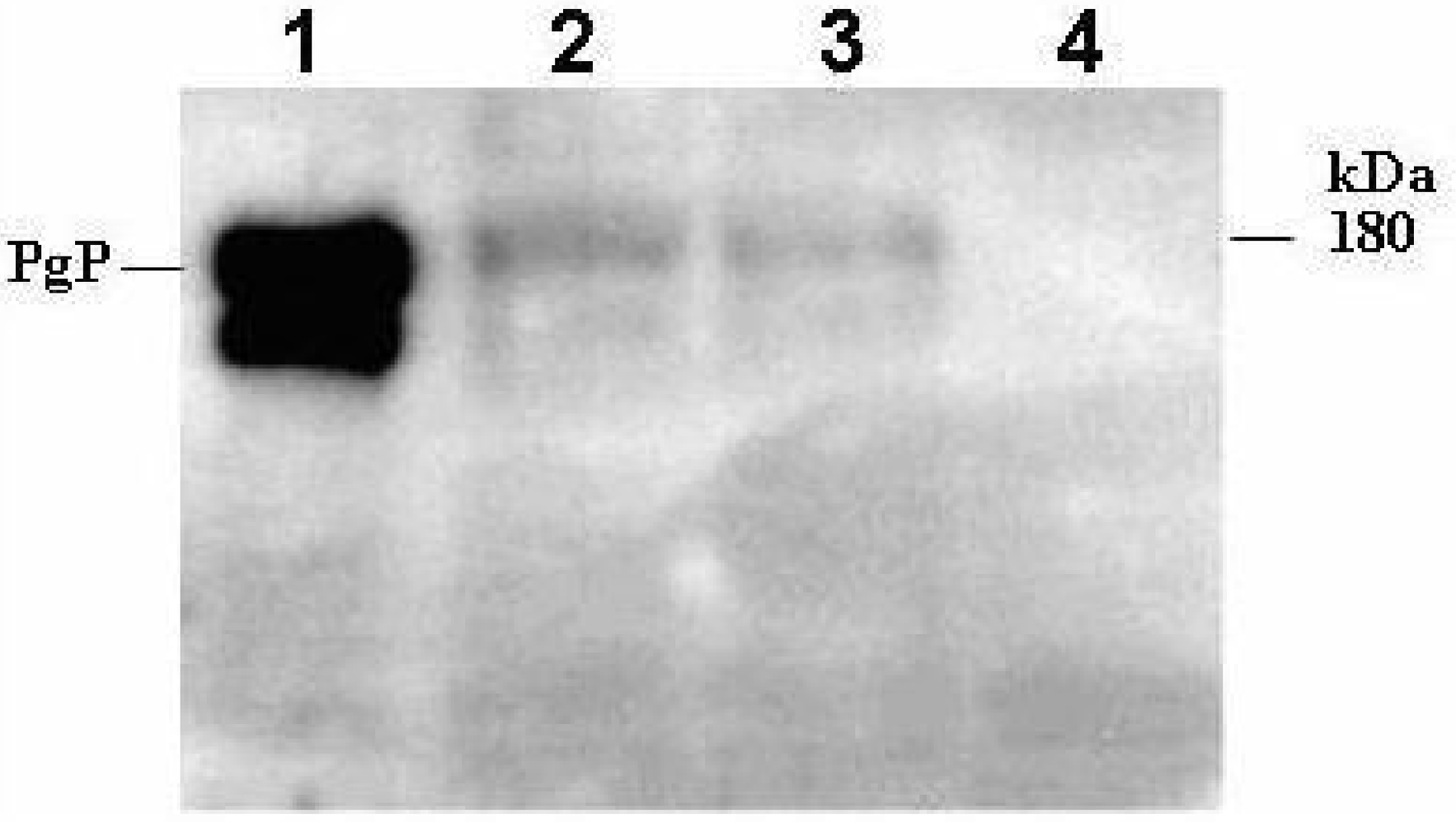

Figure 1

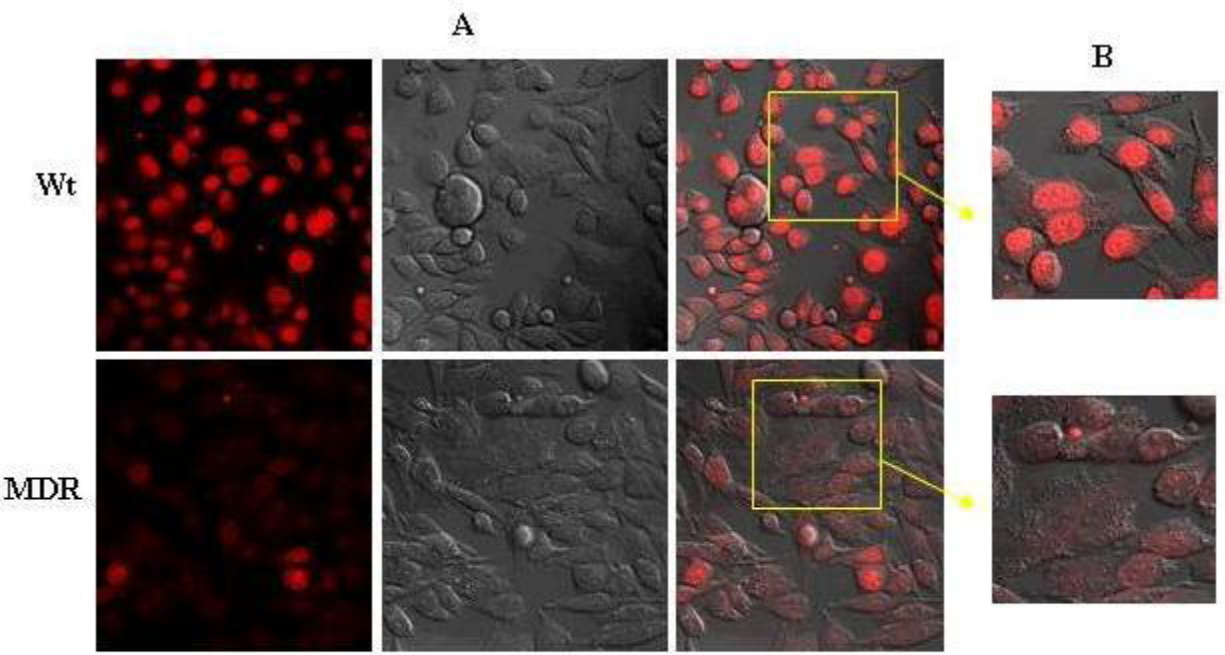

Figure 2

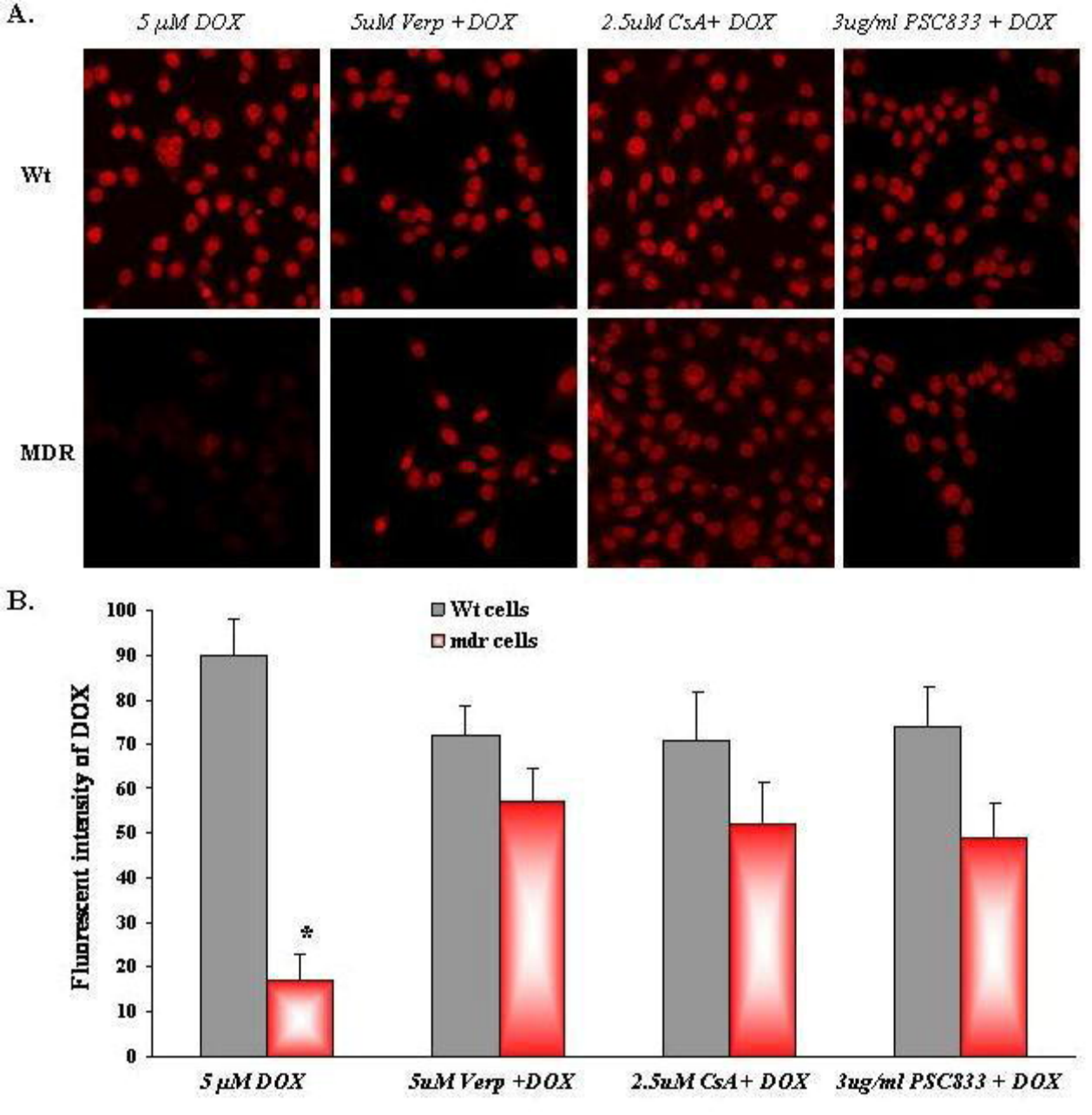
A.
5 μM DOX
5uM Verp +DOX
2.5uM CsA+ DOX
3ug/ml PSC833 + DOX
Wt
MDR
B.
Wt cells
mdr cells
Fluorescent intensity of DOX
100
90
80
70
60
50
40
30
20
10
0
*
5 μM DOX
5uM Verp +DOX
2.5uM CsA+ DOX
3ug/ml PSC833 + DOX

Figure 3

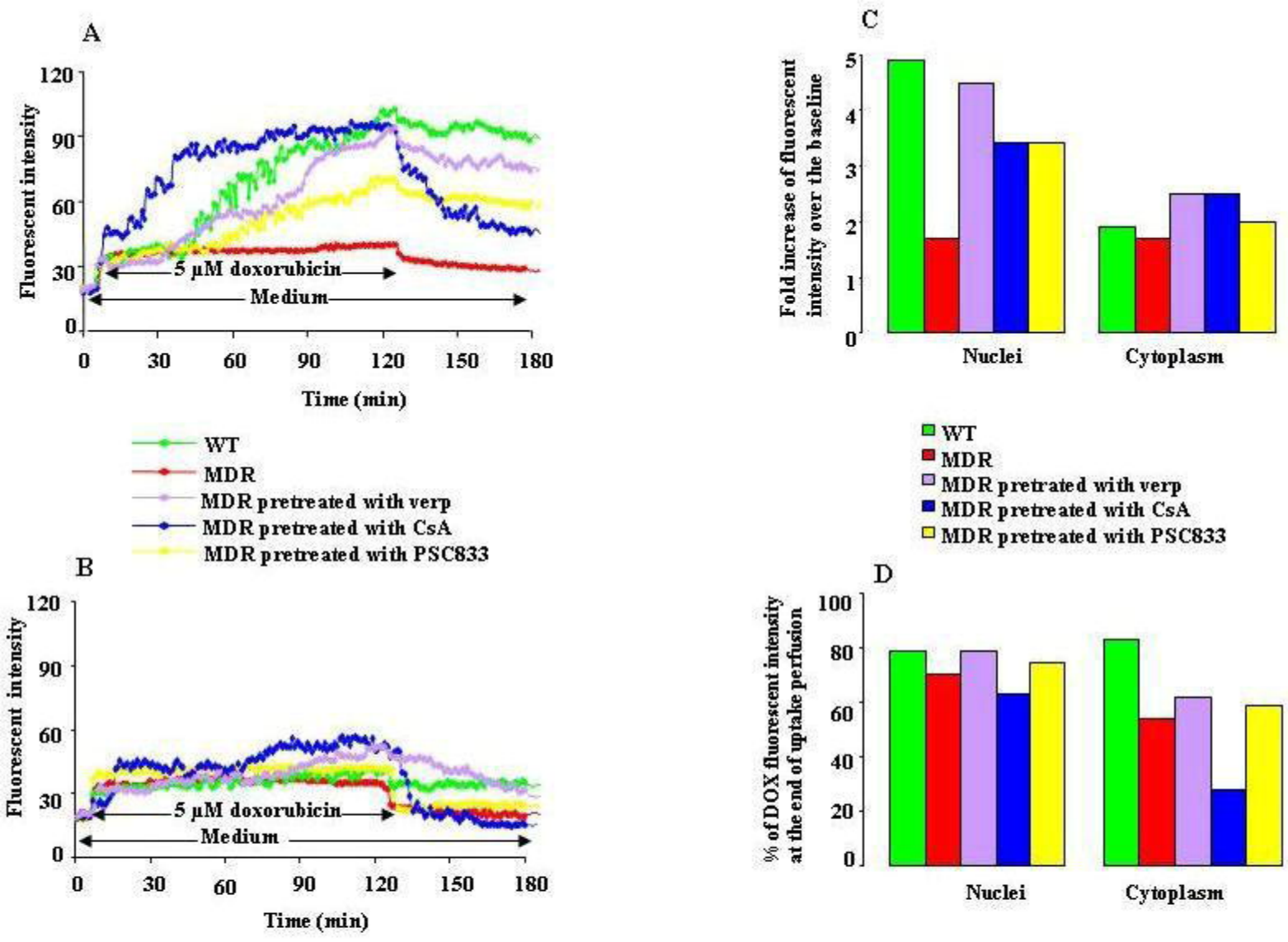

Figure 4

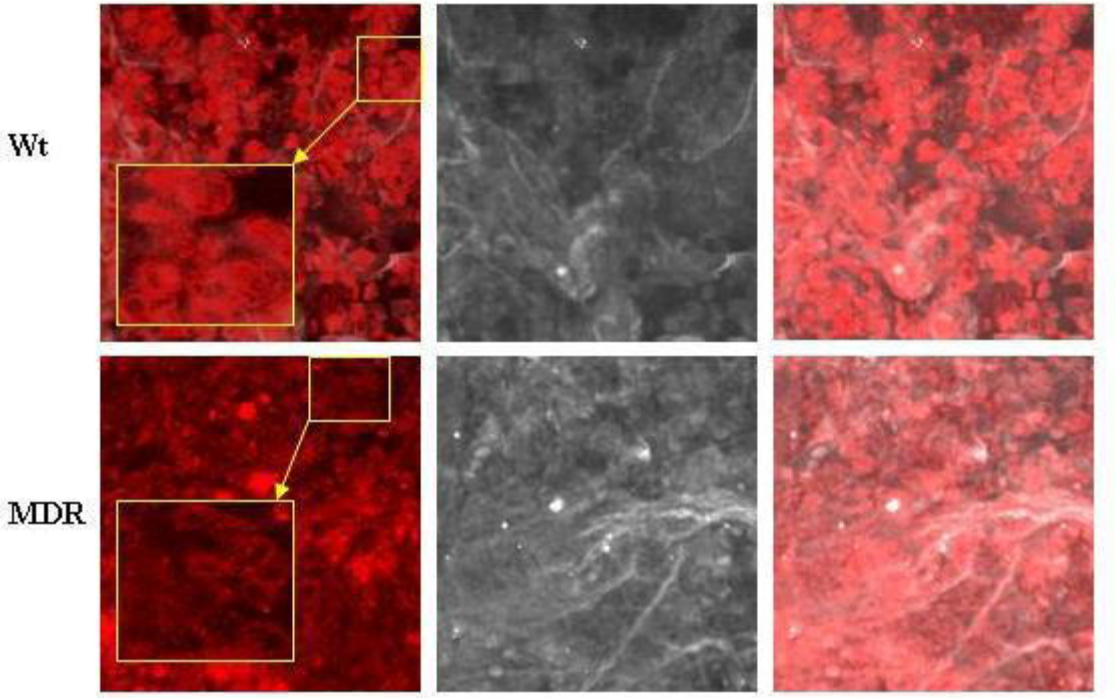

Figure 5

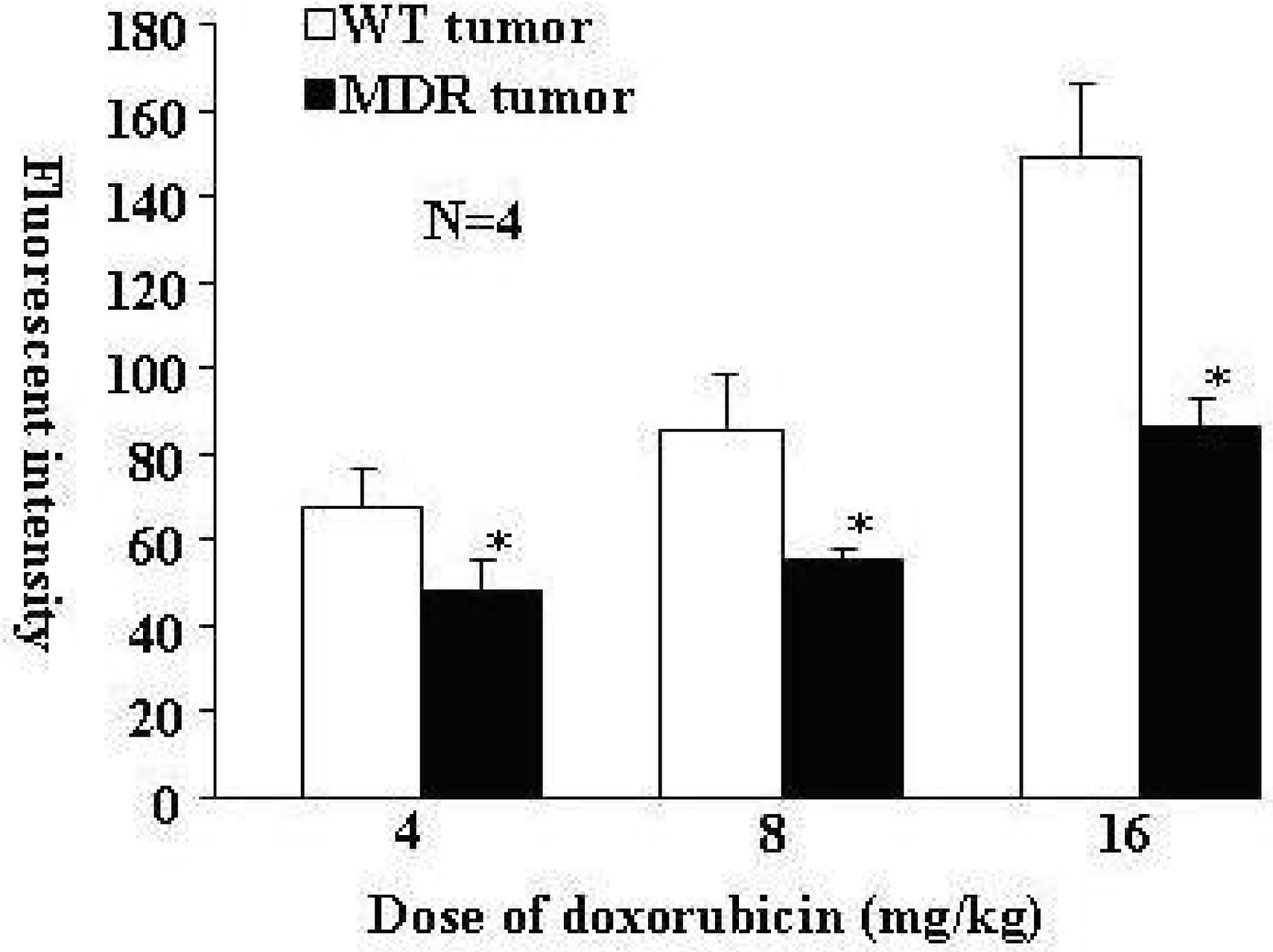
□WT tumor
■MDR tumor
N=4
Fluorescent intensity
180
160
140
120
100
80
60
40
20
0
*
*
*
4
8
16
Dose of doxorubicin (mg/kg)

Figure 6